Human Molecular Genetics, 2013, Vol. 22, No. 22 **4460–4473**
doi:10.1093/hmg/ddt295
Advance Access published on June 28, 2013

Mutations in *LYRM4*, encoding iron–sulfur cluster biogenesis factor ISD11, cause deficiency of multiple respiratory chain complexes

Sze Chern Lim[1,2], Martin Friemel[3], Justine E. Marum[1,2], Elena J. Tucker[1,2], Damien L. Bruno[1,4], Lisa G. Riley[5], John Christodoulou[5,6,7], Edwin P. Kirk[8], Avihu Boneh[1,2,4], Christine M. DeGennaro[9], Michael Springer[9], Vamsi K. Mootha[9,10,11], Tracey A. Rouault[12], Silke Leimkühler[3], David R. Thorburn[1,2,4] and Alison G. Compton[1,2,*]

[1]Murdoch Childrens Research Institute, Royal Children's Hospital, Flemington Road, Parkville, VIC 3052, Australia, [2]Department of Paediatrics, University of Melbourne, Parkville, VIC 3052, Australia, [3]Institute of Biochemistry and Biology, Department of Molecular Enzymology, University of Potsdam, Potsdam 14476, Germany, [4]Victorian Clinical Genetics Services, Royal Children's Hospital, Parkville, VIC 3052, Australia, [5]Genetic Metabolic Disorders Research Unit, Children's Hospital at Westmead, Westmead, NSW 2145, Australia, [6]Discipline of Paediatrics & Child Health and [7]Discipline of Genetic Medicine, University of Sydney, Sydney, NSW 2006, Australia, [8]Department of Medical Genetics, Sydney Children's Hospital, Randwick, NSW 2031, Australia, [9]Department of Systems Biology, Harvard Medical School, Boston, MA 02115, USA, [10]Center for Human Genetic Research and Department of Molecular Biology, Massachusetts General Hospital, Boston, MA 02114, USA, [11]Broad Institute of Harvard and Massachusetts Institute of Technology, Cambridge, MA 02141, USA and [12]Molecular Medicine Program, Eunice Kennedy Shriver National Institute of Child Health and Human Development, National Institutes of Health, Bethesda, MD 20892, USA

Received February 26, 2013; Revised May 16, 2013; Accepted June 20, 2013

Iron–sulfur clusters (ISCs) are important prosthetic groups that define the functions of many proteins. Proteins with ISCs (called iron–sulfur or Fe–S proteins) are present in mitochondria, the cytosol, the endoplasmic reticulum and the nucleus. They participate in various biological pathways including oxidative phosphorylation (OXPHOS), the citric acid cycle, iron homeostasis, heme biosynthesis and DNA repair. Here, we report a homozygous mutation in *LYRM4* in two patients with combined OXPHOS deficiency. *LYRM4* encodes the ISD11 protein, which forms a complex with, and stabilizes, the sulfur donor NFS1. The homozygous mutation (c.203G>T, p.R68L) was identified via massively parallel sequencing of >1000 mitochondrial genes (MitoExome sequencing) in a patient with deficiency of complexes I, II and III in muscle and liver. These three complexes contain ISCs. Sanger sequencing identified the same mutation in his similarly affected cousin, who had a more severe phenotype and died while a neonate. Complex IV was also deficient in her skeletal muscle. Several other Fe–S proteins were also affected in both patients, including the aconitases and ferrochelatase. Mutant ISD11 only partially complemented for an ISD11 deletion in yeast. Our *in vitro* studies showed that the L-cysteine desulfurase activity of NFS1 was barely present when co-expressed with mutant ISD11. Our findings are consistent with a defect in the early step of ISC assembly affecting a broad variety of Fe–S proteins. The differences in biochemical and clinical features between the two patients may relate to limited availability of cysteine in the newborn period and suggest a potential approach to therapy.

*To whom correspondence should be addressed. Tel: +61 383416287; Fax: +61 383416212; Email: alison.compton@mcri.edu.au

INTRODUCTION

Iron–sulfur clusters (ISCs) are biological prosthetic groups that commonly exist in eukaryotes as [2Fe–2S] and [4Fe–4S] clusters (1). Some examples of their common functions include electron transfer in the mitochondrial oxidative phosphorylation (OXPHOS) complexes I, II and III, enzyme catalysis in aconitase 2 of the citric acid cycle and sensing of environmental or intracellular conditions in aconitase 1 (also known as the iron regulatory protein 1) for gene regulation (2,3). Many protein factors are required for the maturation of iron–sulfur (Fe–S) proteins, from the assembly of ISCs which most often starts in mitochondria, to the incorporation of ISCs into target apoproteins. The maturation process has been best studied in yeast, with human counterparts mostly identified through ortholog searches and subsequent functional studies (4–6). Briefly, cysteine desulfurase which is encoded by *NFS1* is involved in delivering sulfur to ISCU, and frataxin (FXN) either delivers iron (7) or allosterically modifies activity of the initial iron–sulfur cluster assembly complex (8). Cluster transfer proteins such as Fe–S protein NUBPL (also known as IND1), GLRX5 and BOLA3 among many others, then insert the ISCs into target apoproteins (3,9,10). The mitochondrial ISC assembly system is also essential for the maturation of Fe–S proteins in the cytosol and nucleus (11–13). Some evidence has suggested that the assembly of ISCs may also be initiated in the nucleus and/or the cytosol (14), where a number of the mitochondrial ISC assembly factors or their extra-mitochondrial isoforms are also present (5,15–18).

Mutations in six mitochondrial ISC assembly factor genes have been implicated in several human disease phenotypes. The abnormal trinucleotide expansion in *FXN* causes Friedreich's ataxia (MIM 229300) (19). *ISCU* mutations cause myopathy with lactic acidosis and exercise intolerance (MIM 255125) (20–22). *NUBPL* mutations cause childhood-onset mitochondrial encephalomyopathy and complex I deficiency (MIM 613621) (23). A mutation in *GLRX5* is responsible for sideroblastic-like anemia and iron overload in an adult patient (MIM 609588) (24). Most recently, *NFU1* and *BOLA3* mutations were reported in neonates with defects in lipoic acid biosynthesis and deficiency of OXPHOS complexes I, II and III (MIM 605711 and 614299) (9,25,26).

ISC biogenesis desulfurase interacting protein 11 kDa (or ISD11 (4)) participates in the mitochondrial ISC assembly pathway by forming a complex with NFS1 (5). In yeast without Isd11p, Nfs1p had normal or even slightly increased desulfurase activity (4), but was prone to aggregation and proteolytic degradation (4,6). In HeLa cells, ISD11 was found in both mitochondria and the nucleus (5), but its role in the nucleus remains unknown. Knocking down *LYRM4* (the gene encoding ISD11) in HeLa cells not only affected Fe–S proteins in mitochondria and the cytosol, but also affected overall iron homeostasis, leading to iron accumulation in the cells (5).

Here, we report a pathogenic *LYRM4* mutation in two cousins from a consanguineous family of Lebanese and Syrian ancestry. The mutation was identified by massively parallel sequencing of over 1000 genes encoding mitochondrial proteins in the proband (27), who had severe neonatal lactic acidosis but recovered and is currently healthy at 20 years of age. Subsequent Sanger sequencing found the same mutation in his affected cousin, who died at 2 months of age. Both patients had a deficiency of the OXPHOS complexes containing ISCs, namely complexes I, II and III, as well as other mitochondrial and cytosolic Fe–S proteins. The striking difference in clinical outcomes could relate to vulnerability in the neonatal period due to limited availability of the sulfur donor cysteine (28), suggesting a possible approach to therapy.

RESULTS

Mitoexome sequencing identified a homozygous *LYRM4* mutation

The entire mtDNA and 1381 nuclear-encoded mitochondrial-associated genes (together, termed the 'MitoExome' genes) were sequenced in DNA from the proband (P1, Fig. 1). We identified 685 single nucleotide variants and short insertions or deletions (indels) and then prioritized results for variants likely to cause a recessively inherited disease. First, we discarded variants common in public databases based on the allele frequency cut-off at 0.005, leaving 18 variants. Variants predicted to severely impact protein function (23) were then prioritized. From the remaining 11 rare and likely deleterious variants, we prioritized for recessive-type inheritance, namely genes containing a homozygous or two heterozygous variants and found only one such variant, a homozygous c.203G>T mutation in *LYRM4*. *LYRM4* encodes the ISD11 protein required for ISC biogenesis and was a strong candidate gene since both P1 and his affected cousin P2 had a deficiency of OXPHOS complexes I, II and III (Table 1), all of which require ISCs for activity.

The *LYRM4* mutation in P1 was validated via Sanger sequencing and also found to be homozygous in his affected cousin P2 (Fig. 2A). The mutation was not reported in dbSNP (29) version 132 or the 1000 genomes project (30) release 20100804 or Exome Variant Server (NHLBI GO Exome Sequencing Project (ESP), Seattle, WA http://eversusgs.washington.edu/EVS/ January 2013). It was also absent from 172 ethnically matched control chromosomes screened using a Sequenom genotyping assay. The mutation was predicted to change the highly conserved Arg68 to a Leucine (p.R68L) (Fig. 2B).

LYRM4 has three RefSeq transcript variants: NM_020408.4 (Variant 1), NM_001164840.1 (Variant 2) and NM_001164841.1 (Variant 3) (Fig. 2A). The first two exons are common to all

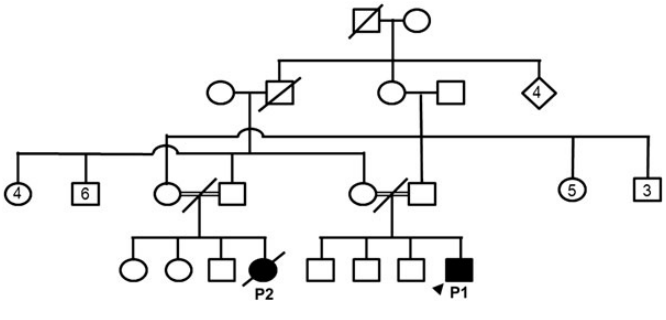

Figure 1. Pedigree of the extended families of patients P1 and P2. P1 and P2 were double first cousins from consanguineous Lebanese/Syrian families. There were at least two consanguineous loops within their parents' sibships with the same degree of consanguinity. Numbers within symbols describe the number of siblings of that gender. The proband is indicated by an arrowhead.

Table 1. Respiratory chain and citrate synthase enzyme activities in skeletal muscle, liver and skin fibroblasts of P1 and P2

	% CI/CS		% CII/CS		% CIII/CS		% CII + III/CS		% CIV/CS		% CS	
	P1	P2	P1	P2	P1	P2	P1	P2	P1	P2	P1	P2
Muscle	**9**	**4**	**10**	**8**	n.t.	**5**	**7**	**14**	58	**11**	201	166
	(70–149)		(80–109)		(31–170)		(80–143)		(76–116)		(66–139)	
Liver	**53**	**3**	**36**	**8**	n.t.	**11**	n.t.	n.t.	81	72	144	218
	(77–124)		(80–126)		(61–136)				(68–132)		(93–107)	
Fibroblasts	64	79	84	181	45	79	48	91	63	112	80	58
	(50–145)		(39–144)		(42–187)		(39–146)		(44–173)		(42–153)	

Respiratory chain enzyme activities are expressed relative to CS as percentage of control mean. CS activity is expressed relative to protein as percentage of control mean. Observed normal ranges are shown in parentheses (mean = 100%) and were determined on 9 (muscle), 6 (liver) or 35 (fibroblast) samples obtained from children lacking evidence of respiratory chain disease. Bold characters indicate values that are deficient relative to protein and relative to the marker enzyme CS. Complex I (CI) is NADH-coenzyme Q1 oxidoreductase, complex II (CII) is succinate-coenzyme Q1 oxidoreductase, complex III (CIII) is decylbenzylquinol-cytochrome *c* oxidoreductase, complex II + III (CII + III) is succinate cytochrome *c* reductase, complex IV (CIV) is cytochrome *c* oxidase. n.t., not tested.

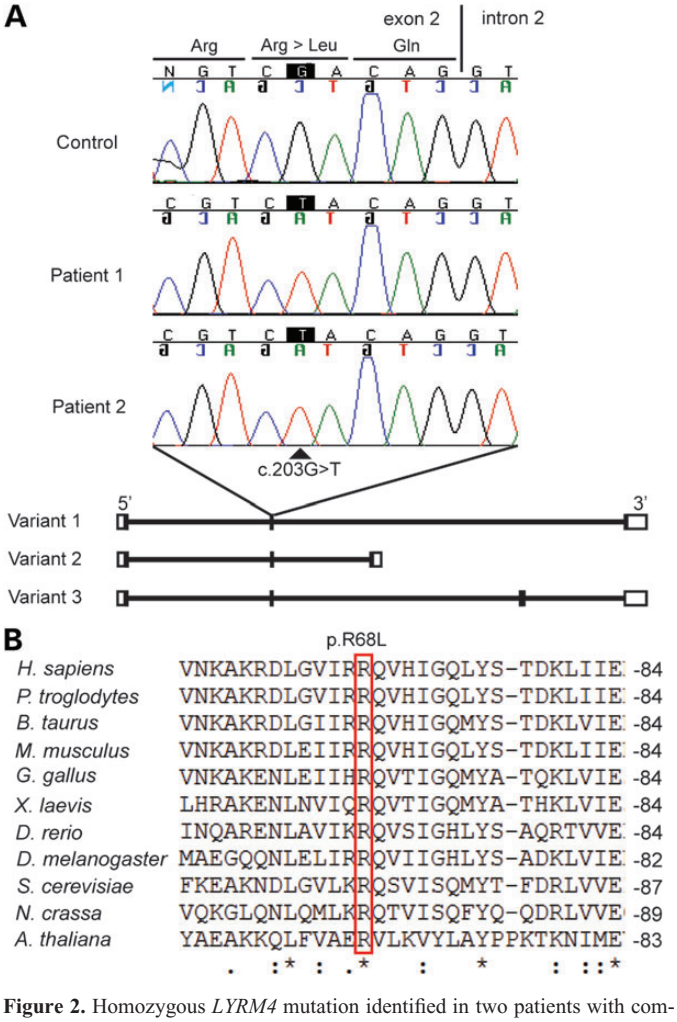

Figure 2. Homozygous *LYRM4* mutation identified in two patients with combined complexes I, II and III OXPHOS deficiency, predicted to affect a highly conserved amino acid residue. (**A**) Chromatograms of Sanger sequencing of gDNA confirmed the homozygous c.203G>T (p.R68L) mutation detected by MitoExome sequencing in P1 and identified the same mutation in P2. This mutation is within exon 2, which is one of the shared exons among all three *LYRM4* transcript variants. (**B**) Arg68 in human ISD11 (NP_065141.3) is highly conserved in vertebrate and invertebrate species shown in the ClustalW2 alignment.

three variants. The mutation is located five bases upstream of the exon2/intron2 boundary. Our work focused on Variant 1, as have all previous relevant publications (4,5,31). Full-length *LYRM4* complementary DNA (cDNA) of Variant 1 was amplified in fibroblasts of both patients treated with or without cycloheximide (Supplementary Material, Fig. S1), suggesting that the mutation did not alter normal splicing or undergo nonsense-mediated mRNA decay, at least in fibroblasts.

MitoExome sequencing also detected a homozygous c.93C>A *COX10* variant in P1 and Sanger sequencing showed that P2 was a heterozygote (Supplementary Material, Fig. S2). This novel variant was also found in 1 of the 172 ethnically matched control chromosomes. *COX10* mutations have been shown to cause isolated complex IV deficiency (32). The c.93C>A variant was predicted to cause a p.D31E change affecting a very poorly conserved residue in vertebrates (33). Given the milder clinical phenotype and normal complex IV activity in P1 who is homozygous for the *COX10* mutation, it seems unlikely that the *COX10* variant is responsible for the more severe phenotype observed in P2.

LYRM4 was within a shared region of Long Contiguous Stretch of Homozygosity

SNP genotyping using the Illumina HumanCytoSNP-12 array identified two shared regions of Long Contiguous Stretch of Homozygosity (LCSH) present in P1 and P2: chr6:4,762,144–11,270,637bp (Fig. 3) and chr21:28,127,764–29,481,474bp (Supplementary Material, Fig. S3). Only three genes from the chromosome 6 region were predicted to encode mitochondrial proteins (*LYRM4*, *FARS2* and *TMEM14C*), and these were all well covered in our MitoExome sequencing at >15× coverage. There were no MitoExome genes in the chromosome 21 region. *LYRM4* was the only candidate gene with prioritized sequence variants.

Levels of ISD11 and proteins with ISCs were severely decreased in patients' muscle and liver

ISD11 was not detectable in P2 skeletal muscle tissue or P1 and P2 liver using sodium dodecyl sulfate-polyacrylamide gel electrophoresis (SDS–PAGE) western blot (Fig. 4). No skeletal

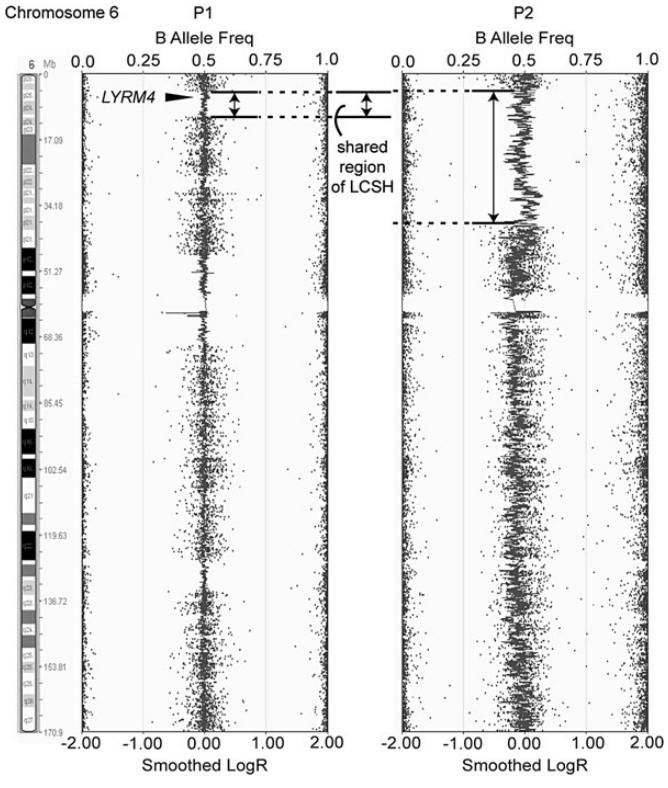

Figure 3. SNP array profiles (Illumina KaryoStudio software) for chromosome 6 of P1 and P2. Frequencies of the B alleles along the chromosomes are indicated, where A and B are arbitrary labels for two alternative alleles. The 'logR' values reflect copy numbers, where 0.00 suggests copy number is equal to 2, whereas <0 and >0, respectively, suggest loss and gain of copy number. *LYRM4* is located within the region of LCSH shared between P1 and P2 on chromosome 6. The deviations in 'logR' values for P2 were genomic waves due to the sub-optimal DNA quality and did not reflect genuine copy number change.

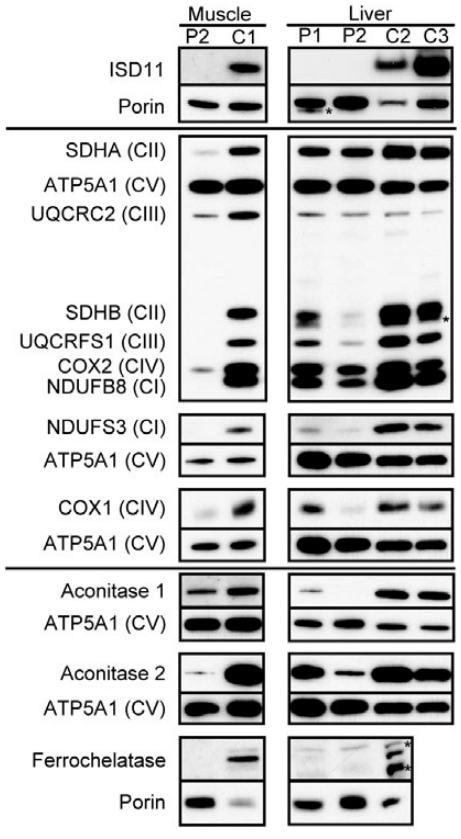

Figure 4. SDS–PAGE western blot panel of patients' muscle and liver samples. In P2 muscle, ISD11 protein was undetectable and protein levels of all complex I–IV subunits investigated were either severely reduced or too low to be detected. In both patient liver samples (P1 and P2), ISD11 protein was undetectable and SDHB and UQCRFS1 levels were most severely reduced. COX1 and COX2 were only reduced in P2 but not in P1 liver. The aconitases and ferrochelatase in patient muscle and liver samples were either not detectable or reduced. C1 was used as muscle control, C2 and C3 as liver controls. P1 muscle sample was not available for analysis. At least one subunit from each OXPHOS complex was investigated: NDUFB8 and NDUFS3 from complex I (CI), SDHA and SDHB from complex II (CII), UQCRC2 and UQCRFS1 from complex III (CIII), COX1 and COX2 from complex IV (CIV), and ATP5A1 from complex V (CV). SDHB, UQCRFS1, aconitase 1 (cytosolic) and 2 (mitochondrial), and ferrochelatase are Fe–S proteins. ATP5A1 and porin were loading controls. Non-specific bands were marked with asterisks. Quantification of proteins was done by densitometry and results are shown in Supplementary Material, Table S1.

muscle biopsy was available from P1 for analysis. ISD11 is essential for ISC biogenesis in yeast (4,6) and in HeLa cells (5). In the OXPHOS system, complexes I, II and III contain subunits with ISCs, such as the complex II subunit SDHB and the complex III subunit Rieske (UQCRFS1). We used protein lysates made from patients' muscle and liver tissues for SDS–PAGE western blot to investigate the relative amounts of OXPHOS subunits compared with controls (Fig. 4, Supplementary Material, Table S1). In P2 muscle, the complex I subunits NDUFB8 and NDUFS3, the complex II subunit SDHB and the complex III subunit UQCRFS1 were all undetectable, while protein levels of the complex II subunit SDHA, complex III subunit UQCRC2 and the complex IV subunits COX2 and COX1 were decreased to 16, 35, 22 and 20% of control, respectively (Fig. 4, Supplementary Material, Table S1). This is consistent with the OXPHOS enzyme activity assay results where P2 muscle had severely reduced activity levels of complexes I–IV (Table 1). For liver samples, subunits of complexes I, II and III, except UQCRC2, were reduced in both patients but the decreases were more pronounced in P2. Of note, the complex IV subunit COX1 was also reduced to 11% of control mean in P2 liver.

SDS–PAGE western blotting was also performed to investigate the amounts of other Fe–S proteins, aconitase 1, aconitase 2 and ferrochelatase (Fig. 4, Supplementary Material, Table S1). Aconitase 1, a cytosolic protein was moderately reduced in P2 muscle, undetectable in P2 liver and reduced to 14% of control mean in P1 liver. Aconitase 2, its mitochondrial isozyme, was reduced to 6 and 19%, respectively, in P2 muscle and liver. The aconitase 2 level in P1 liver was 49% of control mean. Ferrochelatase, a heme biosynthesis enzyme (reviewed in (34)), requires a [2Fe–2S] cluster for stability (35) and was undetectable in P2 muscle and liver, and was barely detected in P1 liver.

Fibroblasts of both patients had normal OXPHOS enzyme activity levels (Table 1). Activity of the pyruvate dehydrogenase complex was also measured in P1 fibroblasts and found to be normal. We hypothesized that transformation of P2 fibroblasts into myotubes using MyoD could unmask an OXPHOS defect, as previously demonstrated for *YARS2* patients (36). This would allow phenotypic correction studies to be performed on

the converted fibroblasts by rescuing with wild-type *LYRM4* cDNA. A successful transformation of control and P2 fibroblasts to myotubes was demonstrated by induction of the skeletal muscle-specific protein α-skeletal actin (Supplementary Material, Fig. S4). However, transformation to myotubes did not unmask an OXPHOS enzyme defect and showed normal amounts of OXPHOS subunit proteins (Supplementary Material, Fig. S4), so this approach could not be used to confirm pathogenicity of the *LYRM4* mutation.

The p.R68L variant failed to fully complement for an isd11 deletion in yeast

To evaluate the effect of the p.R68L mutation in ISD11, we turned to a yeast complementation assay. Two plasmid-borne versions of *S. cerevisiae* were constructed, both containing the endogenous *ISD11* promoter and terminator: one with the wild-type coding sequence (pISD11) and the other with the yeast equivalent of the patient mutation, p.R71L (pISD11R71L). pISD11 and pISD11R71L were transformed into heterozygous *ISD11* deletion (*isd11*Δ) strains and sporulated to create strains where the only copy of *ISD11* was on the plasmid. The fitness consequence of p.R71L was measured by competitive growth assays with a wild-type strain and showed a significant decrease in fitness in all four growth media tested (Fig. 5; $P < 0.02$ from a two-tailed *t*-test for all four media).

The p.R68L variant did not affect the stability of NFS1/ISD11 complex

To further evaluate the functional effect of p.R68L in ISD11, we next analyzed its impact on stability of the NFS1/ISD11 complex. First, both proteins were co-expressed in *Escherichia coli* cells and the complex was purified. Figure 6 shows the chromatograms of the co-purified NFS1Δ1-55/ISD11 and NFS1Δ1-55/ISD11-R68L complexes after size exclusion chromatography. Both complexes were eluted as a complex from the size exclusion column at a molecular mass of ∼145 kDa, which corresponded to a complex consisting of an NFS1 dimer with a stoichiometry of ISD11 subunits of 1:1 or 1:2. An additional peak was eluted which corresponded to the size of an NFS1 monomer. The presence of ISD11 in the complexes was confirmed by SDS–PAGE of the fractions in addition to immunodetection using ISD11 antibodies (data not shown). The NFS1Δ1-55/ISD11-R68L complex was more prone to aggregation compared with the NFS1Δ1-55/ISD11 complex (Fig. 6). Melting temperatures of the complexes were determined by circular dichroism (CD) spectroscopy and revealed comparable values of 61 and 59.5°C for NFS1Δ1-55/ISD11 and NFS1Δ1-55/ISD11-R68L, respectively. Thus, the p.R68L variant in ISD11 did not alter the stability or the oligomerization state of the NFS1/ISD11 complex.

Purified NFS1Δ1-55/ISD11-R68L complex had minimal L-cysteine desulfurase activity

The kinetic constants of NFS1Δ1-55/ISD11 were reported previously as $k_{cat} = 2–2.5\ min^{-1}$ and $K_M = 0.360–0.434$ mM (8,37). L-Cysteine desulfurase activity of purified NFS1Δ1-55/ISD11-R68L was grossly decreased in comparison to NFS1Δ1-55/ISD11 and comparable with the activity of the NFS1Δ1-55 protein purified in the absence of ISD11 (Fig. 7). ISCU and FXN form a quaternary complex with NFS1/ISD11 which doubles the L-cysteine desulfurase activity (8). Therefore, we analyzed the L-cysteine desulfurase activity of the NFS1Δ1-55/ISD11 complex, NFS1Δ1-55/ISD11-R68L complex, and purified

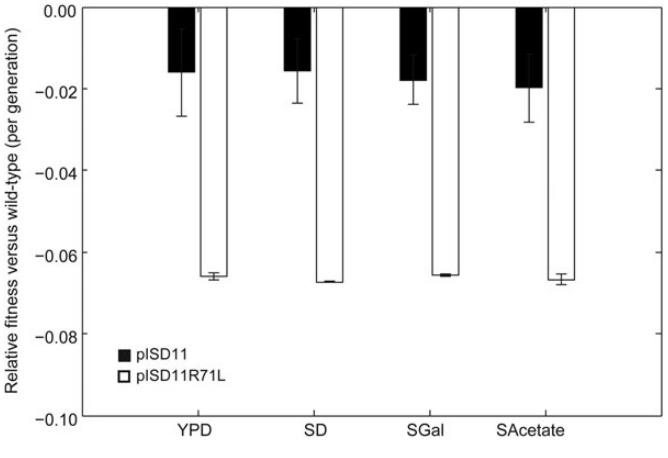

Figure 5. Fitness of the pISD11R71L yeast strain in competitive growth assays. Each bar is the average and standard deviation of three independently generated clones grown in the given media in quadruplicate. All strains were grown in competition with a wild-type strain where ISD11 had not been mutated. The two test strains were deleted for ISD11 and the deletion covered with the given plasmids (deletion and plasmid were generated in a diploid to avoid selection for supressors). Competitive growth was performed in four media: synthetic minimal 2% dextrose (SC), synthetic minimal 2% galactose (SGal), synthetic minimal 2% acetate (SAce) and YPD. Growth differences were measured for 13 generations.

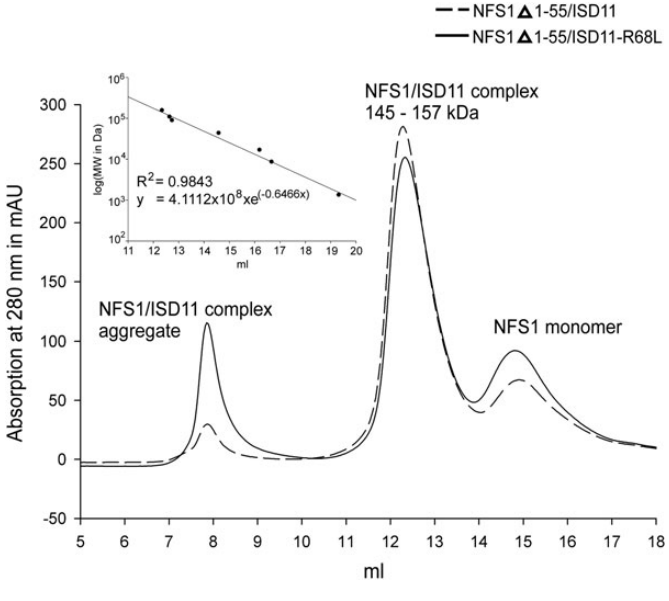

Figure 6. Size exclusion chromatography of co-purified NFS1Δ1-55/ISD11 and NFS1Δ1-55/ISD11-R68L complexes. Complexes containing either NFS1Δ1-55/ISD11 or NFS1Δ1-55/ISD11-R68L eluted at a molecular mass of ∼145 kDa, corresponding to a complex with an NFS1 dimer with a stoichiometry of ISD11 subunits of 1:1 or 1:2. Another eluted peak corresponds to an NFS1 monomer, while the left-most peak corresponds to an aggregate product of the NFS1/ISD11 complex. NFS1/ISD11 labeling refers to complexes of NFS1Δ1-55 with either ISD11 or ISD11-R68L. Inset: Plot of the standard proteins.

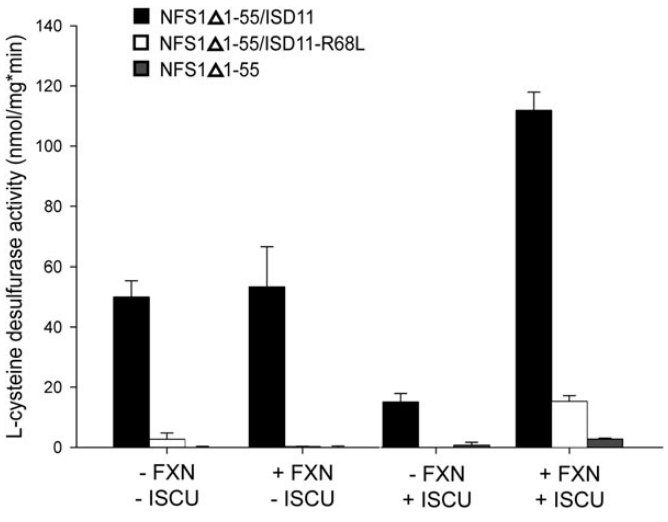

Figure 7. Influence of ISCU and FXN on the L-cysteine desulfurase activity of NFS1Δ1-55/ISD11 and NFS1Δ1-55/ISD11-R68L complexes, and NFS1Δ1-55. L-Cysteine desulfurase activities of NFS1Δ1-55/ISD11 (black), NFS1Δ1-55/ISD11-R68L (white) or NFS1Δ1-55 (grey) were determined in the presence of 1 mM L-cysteine, with or without the addition of ISCU or/and FXN. Desulfurase activity of the NFS1Δ1-55/ISD11 complex (black) was unaffected by FXN alone, decreased 3-fold with ISCU alone, but doubled when both ISCU and FXN were present. Desulfurase activity of the NFS1Δ1-55/ISD11-R68L complex (white) was grossly decreased compared with wild-type complex, and increased when incubated with both ISCU and FXN, but remained deficient compared with the wild-type complex. Purified NFS1Δ1-55 was almost inactive without ISD11 and only attained a detectable residual activity when ISCU and FXN were added to the assay. Data are represented as mean ± standard deviations determined from at least three independent experiments.

NFS1Δ1-55 in the presence or absence of ISCU and/or FXN. Desulfurase activity of the NFS1Δ1-55/ISD11 complex was unaffected by FXN alone, decreased 3-fold with ISCU alone, but doubled when both ISCU and FXN were present, as expected (Fig. 7). The addition of ISCU or FXN alone to the NFS1Δ1-55/ISD11-R68L complex resulted in a slightly decreased L-cysteine desulfurase activity (Fig. 7). However, when the complex was incubated with both ISCU and FXN, its activity increased substantially but remained only ~13% of the activity of the NFS1Δ1-55/ISD11 complex (Fig. 7). In contrast, purified NFS1Δ1-55 was almost inactive without ISD11 and only attained a detectable residual activity when ISCU and FXN were added to the assay (Fig. 7).

Expression of NFS1Δ1-55/ISD11-R68L or NFS1Δ1-55/ISD11 improved the growth of *iscS* mutant to 30% and 85%, respectively

Previously, we showed that the expression of NFS1Δ1-55/ISD11 was able to reduce the growth defect of an *E. coli* strain lacking L-cysteine desulfurase, IscS (37). NFS1 shares 60% amino acid sequence identity with *E. coli* IscS. The growth of *E. coli* cells transformed with different expression plasmids was recorded over 10 h (Fig. 8) and showed that by expressing NFS1Δ1-55/ISD11-R68L, the growth of the *iscS* mutant was improved to ~30% in comparison to the *iscS* mutant transformed with a plasmid expressing IscS. In contrast, cells expressing NFS1Δ1-55/ISD11 were able to restore growth to ~85%.

DISCUSSION

Combined OXPHOS deficiency is one of the most common enzyme defects in patients with OXPHOS disorders, accounting for ~30% of all cases (38). However, in our experience combined deficiency of complexes I, II and III is very rare. Among a cohort of 291 unrelated infantile patients with 'definite' OXPHOS disease that we described previously (27), only six patients other than P1 and P2 had deficient activity of all three complexes relative to citrate synthase (CS) activity. All six were cases of liver enzyme defects and each had a known molecular diagnosis causing hepatic mtDNA depletion or a mtDNA deletion. The complex II defect thus appeared to be secondary to severe liver disease due to the known lability of complex II in such samples (38). In this study we identified mutations in *LYRM4* as a novel cause of deficiency of OXPHOS complexes I, II and III in two Lebanese/Syrian cousins from an extended consanguineous family. This conclusion is based on the following observations: MitoExome sequencing of more than 1000 genes encoding known mitochondrial proteins prioritized a homozygous c.203G>T (p.R68L) *LYRM4* mutation as the only likely deleterious recessive defect in the proband. Independent SNP analyses identified the *LYRM4* gene as one of only three genes encoding known mitochondrial proteins in regions that were identical by descent in the two affected cousins. Sanger sequencing identified the same homozygous mutation in both affected cousins, but the variant was absent from public sequencing databases and from 172 control chromosomes of similar ethnicity. The mutation was predicted to cause a missense change affecting a highly conserved amino acid residue in ISD11, and ISD11 protein was undetectable in patient muscle and liver biopsies. Both affected cousins showed defects in Fe–S proteins, consistent with expectation for a defect in Fe–S biogenesis. Subunits of OXPHOS complexes I, II and III were decreased, particularly SDHB and UQCRFS1 which contain ISCs. The amounts of Fe–S proteins from other biological pathways such as the aconitases and ferrochelatase were also decreased. Furthermore, functional studies of expressed wild-type and mutant proteins showed that (i) in a yeast isd11 deletion strain the mutant protein only partially rescued the growth defect, while (ii) purified NFS1Δ1-55/ISD11-R68L complex had barely detectable L-cysteine desulfurase activity.

While both patients had the same homozygous *LYRM4* mutation, their clinical and biochemical phenotypes were somewhat different. P1 is a healthy 20 year-old man whereas P2 died at 2 months of age. Both patients had combined deficiency of complexes I, II and III in skeletal muscle and liver, but P2 also had complex IV deficiency in skeletal muscle (Table 1). The finding of a c.93C>A *COX10* variant in a homozygous state in P1 but not P2 raised the possibility that these differences could potentially be due to two different genetic disorders segregating in the family. Although rare, there have been reports of patients from consanguineous families where two different disorders are caused by homozygous mutations in two unrelated genes (39). Recessive mutations in *COX10* are known to cause isolated complex IV deficiency (32,40,41). However, we think it is unlikely that the clinical and enzyme differences are related to the *COX10* variant, which affects a poorly conserved amino acid residue and is not predicted to be pathogenic

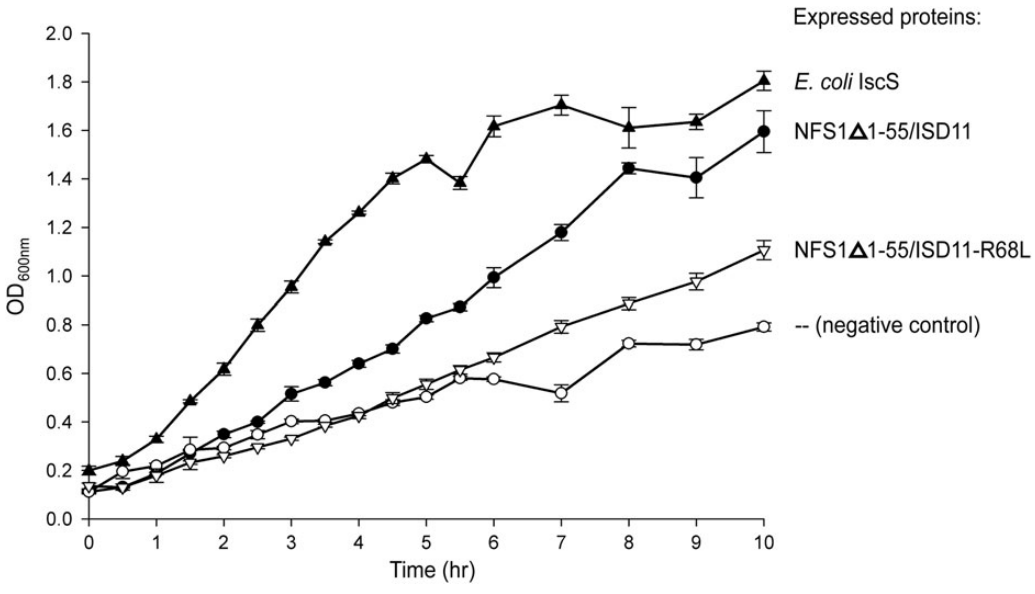

Figure 8. Growth curves of *E. coli* CL100(*ΔiscS*)(DE3) strain transformed with NFS1Δ1-55/ISD11, NFS1Δ1-55/ISD11-R68L and IscS expression plasmids. *E. coli* lacking IscS exhibit a striking growth defect (negative control), which is able to be reversed with the expression of a plasmid containing IscS (*E.coli* IscS). The growth defect was able to be largely rescued by expressing NFS1Δ1-55/ISD11 but cells expressing NFS1Δ1-55/ISD11-R68L showed only a minor improvement in growth. The growth of *E. coli* was recorded by measuring the OD_{600nm} every 30 to 60 min. Data are represented as mean ± standard deviations determined from three independent experiments.

(42,43). Additionally, the c.93C>A *COX10* variant was homozygous in the less severely affected P1 and heterozygous in the more severely affected P2 (Supplementary Material, Fig. S2).

The possible pathogenetic mechanism suggested for patients with *TRMU* mutations (MIM 613070) provides a likely explanation for the differences between our two patients. Zeharia *et al*. reported that most patients with *TRMU* mutations presented at 2–4 months of age and those who survive the neonatal episode remain healthy (28). Sulfur is essential for the function of mitochondrial tRNA-specific 2-thiouridylase 1 (TRMU) (28). The availability of cysteine, the source of sulfur for TRMU activity and ISC biogenesis, is limited during the neonatal period due to low activity of cystathionase, which is essential for the endogenous synthesis of cysteine via the transsulfuration pathway (44). Cystathionase activity increases gradually during the first few months of life (44). Additionally, the level of metallothionein, a cysteine source, is highest at birth but drops rapidly during the first month of life (45). Hence, patients with mutations affecting sulfur-dependent enzymes could be most vulnerable in the first months of life. The clinical outcome of such patients could thus rely on dietary availability of cysteine. It follows that providing a sulfur-donor such as cysteine or N-acetyl cysteine to patients presenting in the first few months of life with symptoms such as primary lactic acidosis or hepatic failure that could potentially be due to mutations in genes such as *LYRM4* or *TRMU* may constitute a novel, practical therapy for these patients.

The identified mutation in *LYRM4* connected to OXPHOS disorders of complexes I, II and III in the two cousins provides new evidence that ISD11 is a crucial part of ISC biosynthesis in humans. Isd11p in yeast has been described as a direct interaction partner of Nfs1p (4,6) and the ISC core complex in humans (31,46). Further investigations revealed that the function of human NFS1 *in vitro* is totally absent without co-expression of ISD11 (8,37) and mutations in conserved amino acid motifs in ISD11 have similar effects (47). We showed that ISD11-R68L was able to form a complex with NFS1, but the purified complex was inactive. Only when ISCU and FXN were present, a residual activity of ∼13% in comparison to the purified wild-type protein was obtained. This suggests that in our *LYRM4* patients, NFS1 has a residual L-cysteine desulfurase activity which is sufficient to retain the viability of the patient, at least in the presence of adequate cysteine supply. The functional complementation of the *E. coli iscS* mutant confirmed these results.

Although the ISD11 antibodies used in our study were able to determine that ISD11 protein was undetectable in both patient skeletal muscle and liver samples, it could not detect ISD11 protein in the fibroblast samples of a control and P2 (Supplementary Material, Fig. S4). It is unclear whether the fibroblasts have a different isoform of ISD11 protein that is not recognized by this antibody. Similar to other patients with ISC assembly defects (9,10,23), the *LYRM4* mutation reported here was not embryonic lethal to humans and specifically affected certain tissues. More work is needed to unveil the redundancy or alternate counterparts of these assembly factors, which account for this tissue variability.

In yeast, Isd11p is essential for ISC biosynthesis in mitochondrial, cytosolic and nuclear proteins (4,6). *LYRM4* knockdown in HeLa cells had detrimental effects on ISC assembly in mitochondria and the cytosol (5). The current working model of ISC assembly for human Fe–S proteins in mitochondrial, cytosolic and nuclear compartments is outlined in Figure 9. ISD11 is involved in the earliest step of ISC biosynthesis in mitochondria. An ISD11 defect would thus be expected to impact on a wide variety of biological pathways requiring Fe–S proteins, in

more than one cellular compartment. This contrasts with the more specific effect on OXPHOS complex I caused by mutation in *NUBPL*, which has a role in the later stage of ISC assembly (23). Our study shows that OXPHOS complexes I, II and III were affected in patients' muscle and liver, not only the subunits containing ISCs, but other subunits from the same complexes as well. This is likely due to loss of overall stability of complexes that lack all necessary subunits and subsequent degradation. Furthermore, protein levels of the aconitases, both mitochondrial and cytosolic forms, and ferrochelatase were reduced. Hence, the defect was hypothesized to impact on the citric acid cycle, cellular iron homeostasis and heme synthesis, respectively.

There are members in the ISC assembly pathway with specialized roles and thus when mutated, would impact on a subset of Fe–S proteins. To illustrate this, both NFU1 and ISCU were suggested to have a similar function as scaffold proteins; however, the former seemed to assemble ISCs that are more specific to lipoate synthesis (9). Our work showed ISD11 is required for the proper function of the OXPHOS complexes I, II and III, as well as the aconitases and ferrochelatase. Further research is needed to discover the possible specialized role(s) of ISD11 in ISC assembly. In mammalian cells, ISD11 as well as a number of other ISC assembly factors such as NFS1, FXN, ISCU and NFU1 are present in mitochondria as well as the nucleus and/or the cytosol (5,15–17,48). However, their exact roles in extra-mitochondrial ISC assembly require further investigation, which will be facilitated by the identification of patients with defects in those proteins.

To our knowledge, all patients with combined deficiency of complexes I, II and III who were molecularly diagnosed had mutations in one of the ISC biogenesis factors ((9,20–22,25,49,50) and the *LYRM4* patients described in this study).

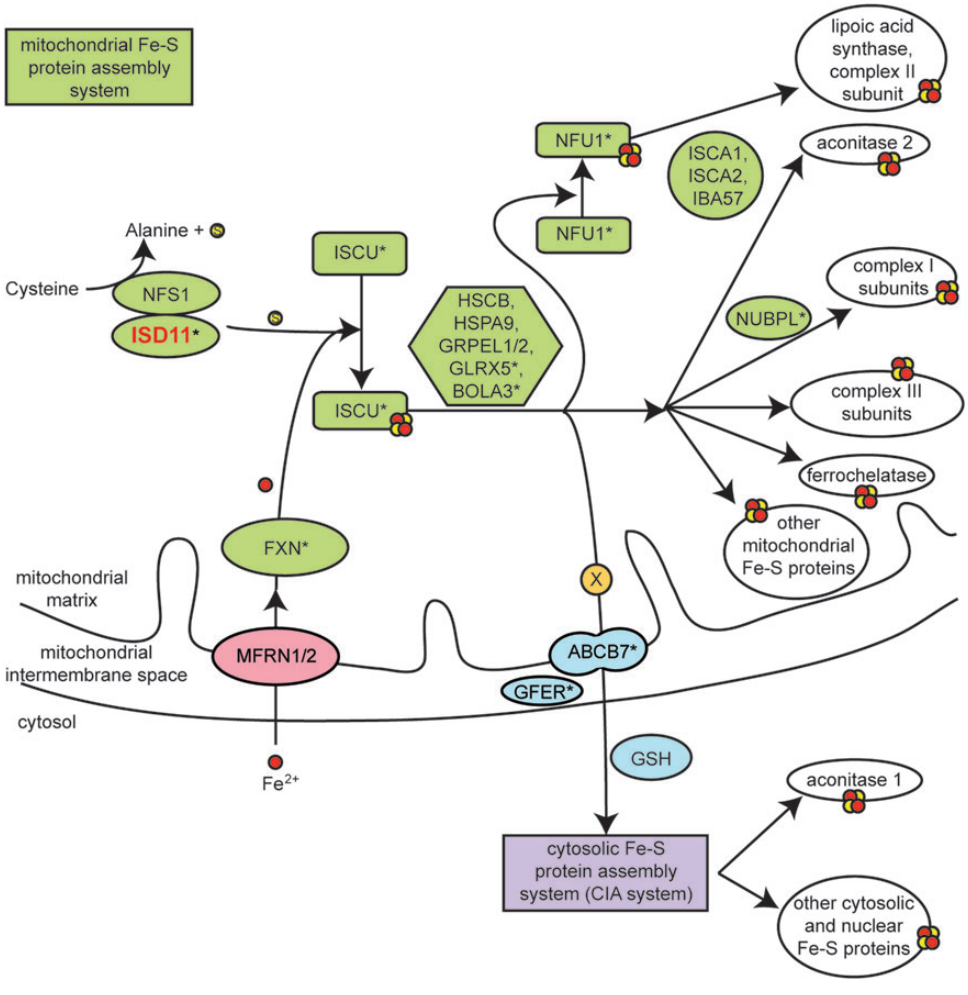

Figure 9. A schematic model of Fe–S protein biosynthesis in the human mitochondria and cytosol. ISD11 forms a complex with NFS1, releasing sulfur (yellow circle) from cysteine. Iron (red circle) is imported from the cytosol facilitated by MFRN1/2 in the mitochondrial inner membrane. Although not fully understood, FXN is thought to be involved in transporting iron to the scaffold protein ISCU, while the NFS1-ISD11 complex delivers the sulfur. FXN also interacts with ISD11, and chaperone proteins HSPA9 (31) and HSCB (67). The clusters are then assembled into target apoproteins by a group of chaperone proteins HSCB, HSPA9 and GRPEL1/2, and GLRX5 with the recently proposed BOLA3 (9). Some Fe–S apoproteins require additional protein factors for ISC insertion, such as aconitase 2, which requires ISCA1, ISCA2 and IBA57, whereas OXPHOS complex I subunits require NUBPL. NFU1 is a specific scaffold protein that functions downstream of ISCU, and is required for ISC insertion in lipoic acid synthase and complex II subunit (25). ISCA1 and IBA57 are also required for this process (68–70). Based on the studies done in yeast, it has been long believed that ABCB7 in the mitochondrial inner membrane plays a role in exporting an unknown product (X) from the mitochondrial ISC system (12,71). This export process is facilitated by GFER and GSH, and is essential for assembly of cytosolic Fe–S proteins. Proteins implicated in human disease are marked with an asterisk. The figure was modified from Sheftel *et al*. (3).

However, not all patients with mutations in ISC biogenesis factors have combined deficiency of complexes I, II and III, such as the *NUBPL* patients with isolated complex I deficiency (23,51) and *NFU1* patients harboring a specific missense mutation with isolated complex II deficiency (25,52). Currently, there are 20 genes with known or predicted roles in mitochondrial ISC biogenesis in humans (3,9) (Table 2). Those genes should be regarded as the top candidate genes for patients with combined deficiency of complexes I, II and III.

MATERIALS AND METHODS

Patient clinical information

Patient 1 (P1, Fig. 1) was born by normal vaginal delivery at 38 weeks of gestation, following an uncomplicated pregnancy. Birth weight was 3170 g. His parents were first cousins of Syrian and Lebanese ancestry. Three siblings were well, and there was no significant family history. Stridor was noted on Day 1 of life, but improved and he was discharged on Day 3. He was admitted to hospital on Day 18 of life because of failure to gain weight (3110 g on admission) and respiratory distress with stridor when upset. He was treated initially with nasopharyngeal continuous positive airway pressure (CPAP), but was intubated on the second day of admission due to worsening respiratory distress, and was transferred to a tertiary referral center. On an initial blood gas he was noted to have a metabolic acidosis with pH 7.14, base excess (BE) −16. Lactic acidosis was evident with a maximum blood lactate of 14.4 mmol/l. Cerebrospinal fluid (CSF) lactate was 3.9 mmol/l. There was evidence of hepatic disease, with abnormal liver enzymes in blood (peak AST 574, ALT 315, GGT 538); however, synthetic function was normal, as was renal function. Clinically he was hypotonic and the cerebral computed tomography scan was normal. Urine screening for amino and organic acid abnormalities showed elevated lactate only. A laryngo-broncho-esophagoscopy (LBO) was performed due to the stridor but was normal. He was extubated following the LBO but deteriorated rapidly, with pH 6.9, BE −18 and was re-intubated. Extubation was successful 12 days after the initial intubation. A barium swallow was performed and showed gastro-esophageal reflux with evidence of barium aspiration.

In the following days, his condition improved and 18 days after admission he was transferred back to the referring hospital. At the time of transfer, he was hypotonic and had continuing stridor, with marked intercostal recession and desaturation with any stimulation. He required nursing in a prone position. He had a weak suck and was almost completely tube fed. Despite adequate calorie intake he had very poor weight gain.

Over the next few weeks he slowly improved with less stridor, improved muscle tone and improved feeding. By Day 52 he was taking occasional bottles well without desaturation; by Day 57 he was fully bottle fed with no stridor. At discharge, aged 65 days, he was fixing and following, was alert and was smilingly responsively. He had continuing hypotonia with a moderate head lag and poor head control when pulled to sit. He had abnormally brisk lower limb reflexes with spread. His weight was 3710 g and head circumference 37.5 cm.

He was lost to follow-up, but the contact was recently re-established and he was reviewed in clinic at age 20 years. He attended a mainstream school and successfully completed 12 years of schooling. He is self-employed, having previously worked as a real estate agent. He participated fully in school sports and has no history of abnormal fatigue or of muscle cramps. His physical examination was normal.

Patient 2 (P2, Fig. 1) was the proband's double first cousin. Labor was induced at 36 weeks gestation because of poor cardiotocography tracings. The birth weight was 2685 g. She developed respiratory distress in the first 24 h of life, and following several episodes of duskiness she was intubated and ventilated. A chest X-ray at the time was suggestive of 'shock lung', and she required mechanical ventilation for 6 days, followed by CPAP for a further 6 days. Supplemental oxygen was required for a total of 5 weeks. A gastric aspirate in the newborn period grew group B Streptococcus, so she was treated with intravenous antibiotics. A urine metabolic screen at 2 days of age showed a moderate increase in lactate, and was only slightly increased a month later.

She was discharged home at 6 weeks of age, but 2 weeks later became lethargic, had a weak cry and poor feeding with weight loss, and was re-admitted. She was noted to have stridor and hepatomegaly. In the ward, she had an episode of respiratory arrest requiring intubation and ventilation and was transferred to a

Table 2. Twenty human genes with known or predicted roles in mitochondrial ISC biogenesis

Gene	Encoded protein	Function	Implicated in human disease?	References
NFS1	NFS1	Sulfur donor	×	
LYRM4	ISD11	In complex with NFS1	√	This study
FDXR[a]	FDXR	Ferredoxin-NADP$^+$ reductase	×	
FDX1[a]	FDX1	Electron transport	×	
FDX1L[a]	FDX1L	Electron transport	×	
SLC25A37	MFRN1	Iron transport	×	
SLC25A28	MFRN2	Iron transport	×	
FXN	FXN	Iron binding and delivery	√	(49,50)
ISCU	ISCU	Scaffold	√	(20–22)
NFU1	NFU1	Specific scaffold protein	√	(9,25)
GLRX5	GLRX5	ISC transfer	√	(24)
BOLA3[a]	BOLA3	ISC transfer	√	(9)
HSPA9[a]	HSPA9	ISC transfer	×	
HSCB[a]	HSCB	ISC transfer	×	
GRPEL1[a]	GRPEL1	ISC transfer	×	
GRPEL2[a]	GRPEL2	ISC transfer	×	
NUBPL	NUBPL	ISC transfer to OXPHOS complex I	√	(23,51)
ISCA1	ISCA1	ISC transfer to radical SAM-dependent proteins and aconitase	×	
ISCA2[a]	ISCA2	ISC transfer to radical SAM-dependent proteins and aconitase	×	
IBA57	IBA57	ISC transfer to radical SAM-dependent proteins and aconitase	×	

[a]Prediction, based on homology screens and/or functional studies. Table was adapted from Sheftel *et al*. (3).

tertiary pediatric hospital. She had a moderate metabolic acidosis with a normal anion gap, but with a blood lactate of 9.3 mmol/l (normal range (19) 0.7–2.0). Her urine metabolic screen showed a gross increase of lactate and severe ketosis.

Despite becoming hemodynamically normal and having a normal cardiac echo, metabolic acidosis and lactic acidemia persisted. CSF lactate was 3.9 mmol/l (NR 0–1.9), plasma lactate was 4.9 mmol/l and blood pyruvate 0.13 mmol/l (NR 0.03–0.10). Electroencephalography showed epileptiform changes. Magnetic resonance imaging of the brain was normal, while proton magnetic resonance spectroscopy revealed a large lactate doublet peak.

Her clinical condition progressively deteriorated and she succumbed at 12 weeks of age. Post mortem muscle histology revealed widened fiber size distribution. There were no ragged red fibers, and cytochrome oxidase staining was normal. The glycogen content was reduced, but there was increased lipid in virtually all muscle fibers. Liver histology showed increased nodulation but no true cirrhosis. There was mild non-inflammatory portal tract expansion, but no significant bile duct proliferation. There was marked micro- and macrovesicular steatosis, mainly in the perivenular regions and mid-zones. The iron content was mildly increased. Hepatocellular glycogen was markedly reduced. On electron microscopy, mitochondria were somewhat swollen and pleomorphic in muscle and liver, most with sparse cristae. There was a loss of mitochondrial dense granules but no crystalline mitochondrial inclusions. Three older children were well.

Mitoexome sequencing and variant prioritization

MitoExome sequencing (massively parallel sequencing of 1381 nuclear genes encoding proteins with mitochondrial location and the entire mtDNA) and variant prioritization have been previously described (27). P1 is listed as P26 in the MitoExome sequencing study (27). The study protocols were approved by the ethics committee at the Royal Children's Hospital, Melbourne. All samples were obtained as part of diagnostic investigations, and families provided informed consent.

Sanger sequencing

DNA isolation, RNA isolation, cDNA synthesis, inhibition of nonsense mediated decay, mRNA splicing and sequencing of PCR products were performed as described previously (23). PCR primers are listed in Supplementary Material, Table S2.

Sequenom genotyping assay

A specifically designed multi-plexed MALDI-TOF mass spectrometry (Sequenom) assay was used to genotype 86 Lebanese controls for the c.203G>T *LYRM4* mutation and c.93C>A *COX10* variant. Genotypes were called by the MassARRAY System Typer version 4.0 software (Sequenom). Details of primers and conditions are available on request.

Molecular karyotyping

Molecular karyotyping of DNA samples was carried out using the Illumina HumanCytoSNP-12 array (version 2.1) as previously described (53). Automated detection of LCSH was performed using the cnvPartition v3.1.6 algorithm in KaryoStudio software. SNP genotypes were generated in GenomeStudio software (Illumina) using data from a set of 102 intra-run samples. DNA samples yielded an SNP call rate of 99.5%. Annotation used the NCBI36/hg18 human genome assembly.

Enzyme and protein analyses

Enzyme assays for respiratory chain complexes, CS and the pyruvate dehydrogenase complex were performed as described previously (54,55) and are summarized in Table 1. For SDS–PAGE, fibroblasts, MyoD-transduced myotubes, and muscle and liver sections were lyzed in SDS/glycerol solubilization buffer (125 mM Tris pH 8.8, 40% glycerol, 4% SDS, 100 mM dithiothreitol (DTT), 0.01% bromophenol blue) (56), containing cOmplete Mini, EDTA-free protease inhibitor cocktail (Roche). Five to twenty micrograms of protein lysates were run on 10% NuPAGE Bis-Tris gels (Invitrogen) and transferred to PVDF membranes (Millipore). The blots were later developed using ECL or ECL Plus detection reagents (Amersham Bioscience).

Primary antibodies for protein detection were: ISD11 (Novus biological, NBP1-79672 or an anti-serum gifted by Gino Cortopassi (31)) that was affinity purified (5), MitoProfile® Total OXPHOS Human WB Antibody Cocktail containing ATP5A1, UQCRC2, SDHB, COX2 and NDUFB8 (MitoSciences, MS601), SDHA (Molecular Probes, A11142), UQCRFS1 (MitoSciences, MS305), NDUFS3 (MitoSciences, MS110), COX1 (MitoSciences, MS404), aconitase 1 (Sigma-Aldrich, SAB2501279), aconitase 2 (MitoSciences, MS793), ATP5A1 (Molecular Probes, A21350), ferrochelatase (abcam, ab55965), porin (Calbiochem, 529534) and α-skeletal actin (Sigma, A2172). Secondary antibodies were goat anti-mouse or swine anti-rabbit IgG/HRP (DakoCytomation, P0447, P0217) and bovine anti-goat IgG/HRP (Jackson Lab Inc., 805-035-180). Quantification of western blots was performed by densitometry measurement using ImageJ software.

MyoD-induced transformation of fibroblasts in myotubes

Production and titration of lentiviral particles containing MyoD, fibroblast transduction and differentiation into myotubes were performed as described previously (57), except that Matrigel was not used.

Evolutionary conservation

Evolutionary conservation of ISD11 was determined by multiple sequence alignment of the human ISD11 protein (NP_065141.3) with its homologs in 10 additional species: *Pan troglodytes* (XP_518217.1), *Bos taurus* (NP_001069774.1), *Mus musculus* (NP_958746.1), *Gallus gallus* (NP_001185817.1), *Xenopus laevis* (NP_001087036.1), *Danio rerio* (NP_001157713.1), *Drosophila melanogaster* (NP_477059.2), *S. cerevisiae* (NP_010968.1), *Neurospora crassa* (XP_964872.2) and *Arabidopsis thaliana* (NP_200930.1) using ClustalW2 software with default parameters.

Yeast strain construction

pISD11R71L (MSD09V) was constructed by isothermal assembly (58) templated with pISD11 and amplified with primers containing the p.R71L mutation. pISD11 was obtained from the MoBY-ORF (59) collection. pISD11R71L was confirmed by sequencing. isd11Δ::GFP-NAT/ISD11 ho Δ::TDHpr-mCherry-HPH/ho (MSE78Y) was constructed by PCR and homologous recombination (60) into MSB89Y, a diploid derivative of FY4 (a prototropic S288c derivative). The deletion was confirmed by colony PCR and inviability of 50% of the haploid spores. pISD11R71L and pISD11 were transformed into MSE78Y and sporulated in the presence of G418 to maintain the plasmid. Mating type was determined, and three independent isd11Δ::GFP-NAT ho Δ::TDHpr-mCherry-HPH pISD11R71L (MSG32-34) and isd11Δ::GFP-NAT ho Δ::TDHpr-mCherry-HPH pISD11 (MSG35-7) strains were kept. FY4 MATa ho Δ::TDHpr-YFP-HPH (MSG30Y) and FY5 MATalpha ho Δ::TDHpr-YFP-HPH (MSG31Y) were constructed in a similar fashion.

Yeast competitive growth assays

Strains MSG32-37 were each co-cultured independently with MSG30Y or MSG31Y. Saturated co-cultures were diluted 1:100 in fresh media and allowed to reach saturation to eliminate history-dependent effects. For each growth assay, strains were seeded in quadruplicate in 96-well format. Each morning, each culture was diluted 1:100. Saturated cultures were diluted 1:10 in water and analyzed on a flow cytometer (LSRII). Between 20 000 and 40 000 cells were counted at each time point for each well. Cells were segmented by fluorescence to determine the number of query and reference strains (61). Competitive growth was performed in four media: synthetic minimal 2% dextrose (SC), synthetic minimal 2% galactose (SGal), synthetic minimal 2% acetate (SAce) and YPD.

Bacterial strains, plasmids, media and growth conditions

E. coli CL100 (*ΔiscS*)(DE3) (62) were used for heterologous expression of the human NFS1Δ1-55 and ISD11 proteins. The vectors pET15b and pACYCDuet-1 were obtained from Novagen. *E. coli* expression cultures were grown in Luria Broth medium under aerobic conditions at 22°C for 16 h. Ampicillin (150 μg/ml), chloramphenicol (50 μg/ml) and isopropyl-β-D-thiogalactoside (IPTG) (100 μM) were used when required.

Cloning, expression, purification and site-directed mutagenesis of human *NFS1* and *LYRM4*

Human His-NFS1Δ1-55 (pZM2) was expressed in the presence or absence of human ISD11 (pZM4) and purified as described previously (37). Human ISCU and FXN were expressed in BL21(DE3) as previously described by Li *et al*. (63,64). For the construction of the ISD11-R68L variant, primers were designed and the base pair exchanges were introduced by PCR mutagenesis and cloned into pACYCDuet-1. The purity of the NFS1/ISD11 complex and the presence of ISD11 were validated by SDS–PAGE and immunoblotting (data not shown).

Size exclusion chromatography

Co-purified NFS1Δ1-55/ISD11 or NFS1Δ1-55/ISD11-R68L (30 μM) were injected in a volume of 500 μl onto a Superdex 200 column (GE Healthcare, 17-5175-01) equilibrated in 50 mM Tris, 200 mM NaCl, 10 mM DTT, 10 μM PLP (pH 8.0). The absorption at 280 nm was recorded. One milliliter fractions were collected and an aliquot of each fraction was taken for SDS–PAGE and immunoblot analysis. Size exclusion chromatography markers (Biorad, 151–1901): gamma globulin (158 kDa), human sulfite oxidase (110 kDa), IscS-dimer (90 kDa), ovalbumin (44 kDa), myoglobin (17 kDa), MoaD (8.7 kDa) and vitamin B12 (1.3 kDa).

L-Cysteine desulfurase activity assays

L-Cysteine desulfurase activities of NFS1Δ1-55/ISD11, NFS1Δ1-55/ISD11-R68L or NFS1Δ1-55 were quantified by the methylene blue method (65) as described previously (37). Assay mixtures in a total volume of 0.8 ml contained 50 mM Tris, 200 mM NaCl, 10 μM PLP, 1 mM DTT (pH 8.0) and 2 μM NFS1Δ1-55/ISD11, NFS1Δ1-55/ISD11-R68L or NFS1Δ1-55. The reactions were initiated by the addition of L-cysteine (0.1–1.0 mM). The standard curve was recorded with sodium sulfide. NFS1Δ1-55 concentrations were determined from the absorbance at 420 nm using the extinction coefficient of 10.9 mM^{-1} cm^{-1} for the native enzyme.

To determine the influence of human ISCU and FXN (FXN_{81-210}) on the L-cysteine desulfurase activity, specific activities of NFS1Δ1-55/ISD11, NFS1Δ1-55/ISD11-R68L or NFS1Δ1-55 were determined in the presence of 6 μM ISCU and/or 4 μM FXN_{81-210} according to the protocol of Tsai and Barondeau (8). The L-cysteine concentration was set to 1 mM for all combinations. The reactions were incubated for 10 min.

Thermal stability using CD spectroscopy

CD spectra of the NFS1Δ1-55/ISD11 and NFS1Δ1-55/ISD11-R68L complexes were recorded in 50 mM HEPES, 1 mM DTT, 100 mM NaCl, pH 7.5 using a concentration of 0.1 mg/ml protein in a 0.1 cm cuvette in a Jasco 715 CD spectrophotometer. The temperature scan was performed at a fixed wavelength of 220 nm and a temperature slope of 1°C per minute in between 10 and 80°C. The melting temperature (T_m) was calculated from the CD values. Data were fitted using Sigma Plot® describing a two state transition of a monomer from a folded to unfolded state, while the heat capacity remained constant.

Functional complementation of the *E. coli* CL100(Δ*iscS*)(DE3) strain

To analyze the influence of the ISD11-R68L variant on the enzyme activity of NFS1, functional complementation of the *E. coli* CL100(Δ*iscS*)(DE3) strain was analyzed as reported previously (37). The *E. coli* strain was either transformed with plasmids expressing NFS1Δ1-55/ISD11 (pZM2 and pZM4), NFS1Δ1-55/ISD11-R68L (pZM2 and pMF33) or *E. coli* IscS (pSL209) (66). *E. coli* CL100(ΔiscS)(DE3) was transformed with expression vectors pET15b or pACYCDuet-1 as negative controls. Cells were grown at 30°C in the presence of IPTG

over a period of 10 h. The corresponding growth curves were recorded by taking the OD_{600nm} every 30 min in the first 6 h and every hour between the following 6–10 h. Each strain was measured in three independent experiments.

Web resources

ClustalW2 protein alignment, http://www.ebi.ac.uk/Tools/phylogeny/clustalw2_phylogeny/, last accessed on 1 July 2013.

Human GenoTyping tools for Sequenom genotyping assay design, https://www.mysequenom.com/Tools, last accessed on 1 July 2013.

Online Mendelian Inheritance in Man (OMIM), http://www.omim.org/, last accessed on 28 June 2013.

Exome Variant Server (NHLBI GO Exome Sequencing Project (ESP), Seattle, WA http://eversusgs.washington.edu/EVS/ January 2013.

SUPPLEMENTARY MATERIAL

Supplementary Material is available at *HMG* online.

ACKNOWLEDGEMENTS

We thank S. Tregoning and W. Salter for enzyme analyses, Dr F. Collins for patient referral, the subjects and their families for their involvement in this study. We thank the Australian Genome Research Facility (AGRF) for running the CytoSNP array and Dr S.T. Cooper for her assistance with the MyoD transformation studies. We thank Dr S.E. Calvo for her collaboration leading to the initial identification of the *LYRM4* mutation and for helpful discussion.

Conflict of Interest statement: The authors declare no conflict of interest.

FUNDING

The authors thank the NHLBI GO Exome Sequencing Project and its ongoing studies which produced and provided exome variant calls for comparison: the Lung GO Sequencing Project (HL-102923), the WHI Sequencing Project (HL-102924), the Broad GO Sequencing Project (HL-102925), the Seattle GO Sequencing Project (HL-102926) and the Heart GO Sequencing Project (HL-103010). This work was supported by a Melbourne Research Scholarship (to S.C.L.), grants and a Principal Research Fellowship from the Australian National Health and Medical Research Council (to D.R.T.), the Victorian Government's Operational Infrastructure Support Program (to D.R.T.) and support from the intramural program of the *Eunice Kennedy Shriver* National Institute of Child Health and Human Development (to T.A.R.), and the Deutsche Forschungsgemeinschaft (to S.L.).

REFERENCES

1. Rouault, T.A. and Tong, W.H. (2008) Iron–sulfur cluster biogenesis and human disease. *Trends Genet.*, **24**, 398–407.
2. Lill, R. (2009) Function and biogenesis of iron–sulphur proteins. *Nature*, **460**, 831–838.
3. Sheftel, A., Stehling, O. and Lill, R. (2010) Iron–sulfur proteins in health and disease. *Trends Endocrinol. Metab.*, **21**, 302–314.
4. Adam, A.C., Bornhovd, C., Prokisch, H., Neupert, W. and Hell, K. (2006) The Nfs1 interacting protein Isd11 has an essential role in Fe/S cluster biogenesis in mitochondria. *EMBO J.*, **25**, 174–183.
5. Shi, Y., Ghosh, M.C., Tong, W.-H. and Rouault, T.A. (2009) Human ISD11 is essential for both iron–sulfur cluster assembly and maintenance of normal cellular iron homeostasis. *Hum. Mol. Genet.*, **18**, 3014–3025.
6. Wiedemann, N., Urzica, E., Guiard, B., Muller, H., Lohaus, C., Meyer, H.E., Ryan, M.T., Meisinger, C., Muhlenhoff, U., Lill, R. *et al.* (2006) Essential role of Isd11 in mitochondrial iron–sulfur cluster synthesis on Isu scaffold proteins. *EMBO J.*, **25**, 184–195.
7. Stemmler, T.L., Lesuisse, E., Pain, D. and Dancis, A. (2010) Frataxin and mitochondrial FeS cluster biogenesis. *J. Biol. Chem.*, **285**, 26737–26743.
8. Tsai, C.L. and Barondeau, D.P. (2010) Human frataxin is an allosteric switch that activates the Fe–S cluster biosynthetic complex. *Biochemistry*, **49**, 9132–9139.
9. Cameron, J.M., Janer, A., Levandovskiy, V., Mackay, N., Rouault, T.A., Tong, W.H., Ogilvie, I., Shoubridge, E.A. and Robinson, B.H. (2011) Mutations in iron–sulfur cluster scaffold genes *NFU1* and *BOLA3* cause a fatal deficiency of multiple respiratory chain and 2-oxoacid dehydrogenase enzymes. *Am. J. Hum. Genet.*, **89**, 486–495.
10. Ye, H. and Rouault, T.A. (2010) Human iron–sulfur cluster assembly, cellular iron homeostasis, and disease. *Biochemistry*, **49**, 4945–4956.
11. Gerber, J., Neumann, K., Prohl, C., Mühlenhoff, U. and Lill, R. (2004) The yeast scaffold proteins Isu1p and Isu2p are required inside mitochondria for maturation of cytosolic Fe/S proteins. *Mol. Cell Biol.*, **24**, 4848–4857.
12. Kispal, G., Csere, P., Prohl, C. and Lill, R. (1999) The mitochondrial proteins Atm1p and Nfs1p are essential for biogenesis of cytosolic Fe/S proteins. *EMBO J.*, **18**, 3981–3989.
13. Lange, H., Lisowsky, T., Gerber, J., Mühlenhoff, U., Kispal, G. and Lill, R. (2001) An essential function of the mitochondrial sulfhydryl oxidase Erv1p/ALR in the maturation of cytosolic Fe/S proteins. *EMBO Rep.*, **2**, 715–720.
14. Rouault, T.A. (2012) Biogenesis of iron–sulfur clusters in mammalian cells: new insights and relevance to human disease. *Dis. Model. Mech.*, **5**, 155–164.
15. Condò, I., Ventura, N., Malisan, F., Tomassini, B. and Testi, R. (2006) A pool of extramitochondrial frataxin that promotes cell survival. *J. Biol. Chem.*, **281**, 16750–16756.
16. Land, T. and Rouault, T.A. (1998) Targeting of a human iron–sulfur cluster assembly enzyme, Nifs, to different subcellular compartments is regulated through alternative AUG utilization. *Mol. Cell*, **2**, 807–815.
17. Tong, W.-H., Jameson, G.N.L., Huynh, B.H. and Rouault, T.A. (2003) Subcellular compartmentalization of human Nfu, an iron–sulfur cluster scaffold protein, and its ability to assemble a [4Fe-4S] cluster. *Proc. Natl. Acad. Sci. U.S.A.*, **100**, 9762–9767.
18. Tong, W.-H. and Rouault, T.A. (2006) Functions of mitochondrial ISCU and cytosolic ISCU in mammalian iron–sulfur cluster biogenesis and iron homeostasis. *Cell Metab.*, **3**, 199–210.
19. Campuzano, V., Montermini, L., Moltò, M.D., Pianese, L., Cossée, M., Cavalcanti, F., Monros, E., Rodius, F., Duclos, F., Monticelli, A. *et al.* (1996) Friedreich's ataxia: autosomal recessive disease caused by an intronic GAA triplet repeat expansion. *Science*, **271**, 1423–1427.
20. Kollberg, G., Tulinius, M., Melberg, A., Darin, N., Andersen, O., Holmgren, D., Oldfors, A. and Holme, E. (2009) Clinical manifestation and a new *ISCU* mutation in iron–sulphur cluster deficiency myopathy. *Brain*, **132**, 2170–2179.
21. Mochel, F., Knight, M.A., Tong, W.-H., Hernandez, D., Ayyad, K., Taivassalo, T., Andersen, P.M., Singleton, A., Rouault, T.A., Fischbeck, K.H. *et al.* (2008) Splice mutation in the iron–sulfur cluster scaffold protein ISCU causes myopathy with exercise intolerance. *Am. J. Hum. Genet.*, **82**, 652–660.
22. Olsson, A., Lind, L., Thornell, L.-E. and Holmberg, M. (2008) Myopathy with lactic acidosis is linked to chromosome 12q23.3–24.11 and caused by an intron mutation in the *ISCU* gene resulting in a splicing defect. *Hum. Mol. Genet.*, **17**, 1666–1672.
23. Calvo, S.E., Tucker, E.J., Compton, A.G., Kirby, D.M., Crawford, G., Burtt, N.P., Rivas, M., Guiducci, C., Bruno, D.L., Goldberger, O.A. *et al.* (2010) High-throughput, pooled sequencing identifies mutations in *NUBPL* and *FOXRED1* in human complex I deficiency. *Nat. Genet.*, **42**, 851–858.
24. Camaschella, C., Campanella, A., De Falco, L., Boschetto, L., Merlini, R., Silvestri, L., Levi, S. and Iolascon, A. (2007) The human counterpart of

zebrafish shiraz shows sideroblastic-like microcytic anemia and iron overload. *Blood*, **110**, 1353–1358.
25. Navarro-Sastre, A., Tort, F., Stehling, O., Uzarska, MA., Arranz, J.A., del Toro, M., Labayru, M.T., Landa, J., Font, A., Garcia-Villoria, J. *et al.* (2011) A fatal mitochondrial disease is associated with defective NFU1 function in the maturation of a subset of mitochondrial Fe–S proteins. *Am. J. Hum. Genet.*, **89**, 656–667.
26. Haack, T.B., Rolinski, B., Haberberger, B., Zimmermann, F., Schum, J., Strecker, V., Graf, E., Athing, U., Hoppen, T., Wittig, I. *et al.* (2012) Homozygous missense mutation in *BOLA3* causes multiple mitochondrial dysfunctions syndrome in two siblings. *J. Inherit. Metab. Dis.*, **36**, 55–62.
27. Calvo, S.E., Compton, A.G., Hershman, S.G., Lim, S.C., Lieber, D.S., Tucker, E.J., Laskowski, A., Garone, C., Liu, S., Jaffe, D.B. *et al.* (2012) Molecular diagnosis of infantile mitochondrial disease with targeted next-generation sequencing. *Sci. Transl. Med.*, **4**, 118ra10.
28. Zeharia, A., Shaag, A., Pappo, O., Mager-Heckel, A.-M., Saada, A., Beinat, M., Karicheva, O., Mandel, H., Ofek, N., Segel, R. *et al.* (2009) Acute infantile liver failure due to mutations in the TRMU gene. *Am. J. Hum. Genet.*, **85**, 401–407.
29. Sherry, S.T., Ward, M.H., Kholodov, M., Baker, J., Phan, L., Smigielski, E.M. and Sirotkin, K. (2001) dbSNP: the NCBI database of genetic variation. *Nucleic Acids Res.*, **29**, 308–311.
30. The 1000 Genomes Project Consortium (2010) A map of human genome variation from population-scale sequencing. *Nature*, **467**, 1061–1073.
31. Shan, Y., Napoli, E. and Cortopassi, G. (2007) Mitochondrial frataxin interacts with ISD11 of the NFS1/ISCU complex and multiple mitochondrial chaperones. *Hum. Mol. Genet.*, **16**, 929–941.
32. Valnot, I., von Kleist-Retzow, J.C., Barrientos, A., Gorbatyuk, M., Taanman, J.W., Mehaye, B., Rustin, P., Tzagoloff, A., Munnich, A. and Rötig, A. (2000) A mutation in the human heme A:farnesyltransferase gene (*COX10*) causes cytochrome *c* oxidase deficiency. *Hum. Mol. Genet.*, **9**, 1245–1249.
33. Blanchette, M., Kent, W.J., Riemer, C., Elnitski, L., Smit, A.F., Roskin, K.M., Baertsch, R., Rosenbloom, K., Clawson, H., Green, E.D. *et al.* (2004) Aligning multiple genomic sequences with the threaded blockset aligner. *Genome Res.*, **14**, 708–715.
34. Dailey, H.A., Dailey, T.A., Wu, C.K., Medlock, A.E., Wang, K.F., Rose, J.P. and Wang, B.C. (2000) Ferrochelatase at the millennium: structures, mechanisms and [2Fe-2S] clusters. *Cell Mol. Life Sci.*, **57**, 1909–1926.
35. Crooks, D.R., Ghosh, M.C., Haller, R.G., Tong, W.H. and Rouault, T.A. (2010) Posttranslational stability of the heme biosynthetic enzyme ferrochelatase is dependent on iron availability and intact iron–sulfur cluster assembly machinery. *Blood*, **115**, 860–869.
36. Riley, L.G., Cooper, S., Hickey, P., Rudinger-Thirion, J., McKenzie, M., Compton, A., Lim, S.C., Thorburn, D., Ryan, M.T., Giegé, R. *et al.* (2010) Mutation of the mitochondrial tyrosyl-tRNA synthetase gene, YARS2, causes myopathy, lactic acidosis, and sideroblastic anemia–MLASA syndrome. *Am. J. Hum. Genet.*, **87**, 52–59.
37. Marelja, Z., Stöcklein, W., Nimtz, M. and Leimkühler, S. (2008) A novel role for human Nfs1 in the cytoplasm: Nfs1 acts as a sulfur donor for MOCS3, a protein involved in molybdenum cofactor biosynthesis. *J. Biol. Chem.*, **283**, 25178–25185.
38. Thorburn, D.R., Chow, C.W. and Kirby, D.M. (2004) Respiratory chain enzyme analysis in muscle and liver. *Mitochondrion*, **4**, 363–375.
39. Mancuso, M., Filosto, M., Tsujino, S., Lamperti, C., Shanske, S., Coquet, M., Desnuelle, C. and DiMauro, S. (2003) Muscle glycogenosis and mitochondrial hepatopathy in an infant with mutations in both the myophosphorylase and deoxyguanosine kinase genes. *Arch. Neurol.*, **60**, 1445–1447.
40. Antonicka, H., Leary, S.C., Guercin, G.-H., Agar, J.N., Horvath, R., Kennaway, N.G., Harding, C.O., Jaksch, M. and Shoubridge, E.A. (2003) Mutations in *COX10* result in a defect in mitochondrial heme A biosynthesis and account for multiple, early-onset clinical phenotypes associated with isolated COX deficiency. *Hum. Mol. Genet.*, **12**, 2693–2702.
41. Coenen, M.J.H., van den Heuvel, L.P., Ugalde, C., ten Brinke, M., Nijtmans, L.G.J., Trijbels, F.J.M., Beblo, S., Maier, E.M., Muntau, A.C. and Smeitink, J.A.M. (2004) Cytochrome c oxidase biogenesis in a patient with a mutation in *COX10* gene. *Ann. Neurol.*, **56**, 560–564.
42. Adzhubei, I.A., Schmidt, S., Peshkin, L., Ramensky, V.E., Gerasimova, A., Bork, P., Kondrashov, A.S. and Sunyaev, S.R. (2010) A method and server for predicting damaging missense mutations. *Nat. Methods*, **7**, 248–249.
43. Kumar, P., Henikoff, S. and Ng, P.C. (2009) Predicting the effects of coding non-synonymous variants on protein function using the SIFT algorithm. *Nat. Protoc.*, **4**, 1073–1081.
44. Zlotkin, S.H. and Anderson, G.H. (1982) The development of cystathionase activity during the first year of life. *Pediatr. Res.*, **16**, 65–68.
45. Zlotkin, S.H. and Cherian, M.G. (1988) Hepatic metallothionein as a source of zinc and cysteine during the first year of life. *Pediatr. Res.*, **24**, 326–329.
46. Schmucker, S., Martelli, A., Colin, F., Page, A., Wattenhofer-Donzé, M., Reutenauer, L. and Puccio, H. (2011) Mammalian frataxin: an essential function for cellular viability through an interaction with a preformed ISCU/NFS1/ISD11 iron-sulfur assembly complex. *PLoS One*, **6**, e16199.
47. Pandey, A., Yoon, H., Lyver, E.R., Dancis, A. and Pain, D. (2011) Isd11p protein activates the mitochondrial cysteine desulfurase Nfs1p protein. *J. Biol. Chem.*, **286**, 38242–38252.
48. Tong, W.-H. and Rouault, T. (2000) Distinct iron–sulfur cluster assembly complexes exist in the cytosol and mitochondria of human cells. *EMBO J.*, **19**, 5692–5700.
49. Rötig, A., de Lonlay, P., Chretien, D., Foury, F., Koenig, M., Sidi, D., Munnich, A. and Rustin, P. (1997) Aconitase and mitochondrial iron–sulphur protein deficiency in friedreich ataxia. *Nat. Genet.*, **17**, 215–217.
50. Schapira, A.H.V. (2006) Mitochondrial disease. *Lancet*, **368**, 70–82.
51. Tenisch, E.V., Lebre, A.S., Grevent, D., de Lonlay, P., Rio, M., Zilbovicius, M., Funalot, B., Desguerre, I., Brunelle, F., Rötig, A. *et al.* (2012) Massive and exclusive pontocerebellar damage in mitochondrial disease and *NUBPL* mutations. *Neurology*, **79**, 391.
52. Ferrer-Cortès, X., Font, A., Bujan, N., Navarro-Sastre, A., Matalonga, L., Arranz, J., Riudor, E., Toro, M., Garcia-Cazorla, A., Campistol, J. *et al.* (2012) Protein expression profiles in patients carrying *NFU1* mutations. Contribution to the pathophysiology of the disease. *J. Inherit. Metab. Dis.*, 1–7. doi:10.1007/s10545-012-9565-z.
53. Bruno, D.L., White, S.M., Ganesamoorthy, D., Burgess, T., Butler, K., Corrie, S., Francis, D., Hills, L., Prabhakara, K., Ngo, C. *et al.* (2011) Pathogenic aberrations revealed exclusively by single nucleotide polymorphism (SNP) genotyping data in 5000 samples tested by molecular karyotyping. *J. Med. Genet.*, **48**, 831–839.
54. Kirby, D.M., Crawford, M., Cleary, M.A., Dahl, H.H., Dennett, X. and Thorburn, D.R. (1999) Respiratory chain complex I deficiency: an underdiagnosed energy generation disorder. *Neurology*, **52**, 1255–1264.
55. Rahman, S., Blok, R.B., Dahl, H.H.M., Danks, D.M., Kirby, D.M., Chow, C.W., Christodoulou, J. and Thorburn, D.R. (1996) Leigh syndrome: clinical features and biochemical and DNA abnormalities. *Ann. Neurol.*, **39**, 343–351.
56. Cooper, S.T., Lo, H.P. and North, K.N. (2003) Single section western blot: improving the molecular diagnosis of the muscular dystrophies. *Neurology*, **61**, 93–97.
57. Cooper, S.T., Kizana, E., Yates, J.D., Lo, H.P., Yang, N., Wu, Z.H., Alexander, I.E. and North, K.N. (2007) Dystrophinopathy carrier determination and detection of protein deficiencies in muscular dystrophy using lentiviral MyoD-forced myogenesis. *Neuromuscul. Disord.*, **17**, 276–284.
58. Gibson, D.G., Young, L., Chuang, R.-Y., Venter, J.C., Hutchison, C.A. and Smith, H.O. (2009) Enzymatic assembly of DNA molecules up to several hundred kilobases. *Nat. Methods*, **6**, 343–345.
59. Ho, C.H., Magtanong, L., Barker, S.L., Gresham, D., Nishimura, S., Natarajan, P., Koh, J.L.Y., Porter, J., Gray, C.A., Andersen, R.J. *et al.* (2009) A molecular barcoded yeast ORF library enables mode-of-action analysis of bioactive compounds. *Nat. Biotechnol.*, **27**, 369–377.
60. Longtine, M.S., McKenzie Iii, A., Demarini, D.J., Shah, N.G., Wach, A., Brachat, A., Philippsen, P. and Pringle, J.R. (1998) Additional modules for versatile and economical PCR-based gene deletion and modification in *Saccharomyces cerevisiae*. *Yeast*, **14**, 953–961.
61. Springer, M., Weissman, J.S. and Kirschner, M.W. (2010) A general lack of compensation for gene dosage in yeast. *Mol. Syst. Biol.*, **6**, 368.
62. Lauhon, C.T. and Kambampati, R. (2000) The *iscS* gene in *Escherichia coli* is required for the biosynthesis of 4-thiouridine, thiamin, and NAD. *J. Biol. Chem.*, **275**, 20096–20103.
63. Li, K., Tong, W.H., Hughes, R.M. and Rouault, T.A. (2006) Roles of the mammalian cytosolic cysteine desulfurase, ISCS, and scaffold protein, ISCU, in iron–sulfur cluster assembly. *J. Biol. Chem.*, **281**, 12344–12351.
64. Xia, H., Cao, Y., Dai, X., Marelja, Z., Zhou, D., Mo, R., Al-Mahdawi, S., Pook, M.A., Leimkühler, S., Rouault, T.A. *et al.* (2012) Novel frataxin isoforms may contribute to the pathological mechanism of friedreich ataxia. *PLoS One*, **7**, e47847.
65. Fogo, J.K. and Popowsky, M. (1949) Spectrophotometric determination of hydrogen sulfide. *Anal. Chem.*, **21**, 732–734.

66. Leimkühler, S. and Rajagopalan, K.V. (2001) A sulfurtransferase is required in the transfer of cysteine sulfur in the *in vitro* synthesis of molybdopterin from precursor Z in *Escherichia coli*. *J. Biol. Chem.*, **276**, 22024–22031.
67. Shan, Y. and Cortopassi, G. (2011) HSC20 Interacts with Frataxin and is involved in iron–sulfur cluster biogenesis and iron homeostasis. *Hum. Mol. Genet.*, **21**, 1457–1469.
68. Gelling, C., Dawes, I.W., Richhardt, N., Lill, R. and Mühlenhoff, U. (2008) Mitochondrial Iba57p is required for Fe/S cluster formation on aconitase and activation of radical SAM enzymes. *Mol. Cell Biol.*, **28**, 1851–1861.
69. Song, D., Tu, Z. and Lee, F.S. (2009) Human ISCA1 interacts with IOP1/NARFL and functions in both cytosolic and mitochondrial iron–sulfur protein biogenesis. *J. Biol. Chem.*, **284**, 35297–35307.
70. Mühlenhoff, U., Richter, N., Pines, O., Pierik, A.J. and Lill, R. (2011) Specialized function of yeast Isa1 and Isa2 proteins in the maturation of mitochondrial [4Fe–-4S] proteins. *J. Biol. Chem.*, **286**, 41205–41216.
71. Miao, R., Kim, H., Koppolu, U.M.K., Ellis, E.A., Scott, R.A. and Lindahl, P.A. (2009) Biophysical characterization of the iron in mitochondria from ATM1p-depleted *Saccharomyces cerevisiae*. *Biochemistry*, **48**, 9556–9568.